Climate Dynamics (1997) 13: 649–666

Climate Dynamics

Climatology of Northern Hemisphere blocking in the ECHAM model

S. Tibaldi*, F. D'Andrea, E. Tosi[1], E. Roeckner[2]**

[1] Atmospheric Dynamics Group, Department of Physics, University of Bologna, Italy
[2] Max-Planck-Institut für Meteorologie, Hamburg, Germany

Received: 5 July 1996 / Accepted: 14 April 1997

Abstract. An analysis of blocking events is conducted on the output of four integrations of the ECHAM3 atmospheric general circulation model with different configurations of horizontal spectral truncation and oceanic surface temperatures. The definition of local blocking and sector blocking is obtained by using an objective index based on a measure of the local zonality of the flow. Model variability and systematic errors are assessed and frequency diagrams of different quantities relative to blocking statistical and synoptic properties are produced. Effects of resolution and of physical parametrizations on model performance are considered. All versions of the model show a tendency to underestimate blocking occurrence. Evidence of a different nature of the blocking phenomenon in the Euro-Atlantic and in the Pacific sectors is found. The two sectors are characterized by a different sensitivity of blocking frequency to SST prescription, by a different annual cycle and by a different sensitivity of the distribution of blocking lifetime to model resolution. Euro-Atlantic blocking is found to be more the result of internal dynamics of the flow, while Pacific blocking appears more dependent on the oceanic boundary conditions.

1 Introduction

The comparatively large number of recent works dealing with the performances of long and medium range numerical weather prediction (NWP) models in forecasting blocking episodes, onset and maintenance is a symptom of the fact that this phenomenon still represents a problem for atmospheric models.

Blocking was first synoptically defined in the classical works of Rex (1950a, b). Rex's criteria have been often (but not substantially) revised in more recent times by many diagnostic and theoretical papers. A satisfactory and universally accepted theoretical formulation of the mechanisms of blocking onset and maintenance is still lacking. Earlier works (e.g. Tung and Lindzen 1979) attempted an explanation of the phenomenon in terms of Rossby wave resonance on topography or thermal contrast. Since then, many works have addressed the subject with some success in describing particular aspects of the problem; Frederiksen (1982) showed the importance of baroclinic instability in the onset of the block, while works like Green (1977) and Shutts (1983) recognized the eddy transfer of vorticity as an important mechanism for its maintenance. Another group of works (McWilliams 1980; Haines and Marshall 1987) has focused on non-linear stationary solutions, called modons, of the quasi-geostrophic barotropic or equivalent barotropic vorticity equation. The eddy transfer can also be seen as the mechanism that maintains modons against dissipation. Finally, another line of thought must be mentioned which deals with multiple stationary or quasi-stationary solutions of simplified models, one of which was found to resemble a blocking situation (e.g. Charney and DeVore 1979; Vautard and Legras 1988). From these and later works the concept of 'weather regimes' has been introduced and studied. For more complete reviews of blocking theories, see e.g. Bengtsson (1980), Benzi et al. (1986), Hollingsworth et al. (1986), or Kaas (1992).

In addition to the work by Tibaldi and Molteni (1990, hereafter referred to as TM) from which this study draws several basic techniques, examples of works that show the importance of blocking in limiting the usefulness of long and medium range predictions can be found in Tracton et al. (1989), Tracton (1990), Miyakoda and Sirutis (1990), Brankovic and Ferranti (1991), Anderson (1993), and Tibaldi et al. (1994) and (1995).

Blocking however is a critical phenomenon not only for NWP models. Due to its persistent nature and to its large impact on local and hemispheric flow patterns, it is also a very relevant phenomenon in determining the climatology of a region, influencing for example precipitation

Correspondence to: E. Tosi

Current affiliations:
* ARPA-SMR, Servizio Meteorologico Regionale, Bologna, Italy
** Laboratoire de Meteorologie Dynamique du CNRS, Paris, France

anomalies (and consequently shorter-lived drought occurrences). Thus it can be expected that a difficulty in its reproduction may also affect the performance of general circulation models (GCMs) used for simulation of present climate, as well as those used for climate impact studies. An introductory general discussion about the potential of the use of blocking as a diagnostic tool for climate models can be found in Tibaldi (1993), the ideas of which are to some extent applied and extended in the present work.

The analysis of blocking simulation in climate models has an interest of a somewhat different nature than in NWP models, where the main concern is the lack of predictability linked to the blocking onset and decay. Moreover, Anderson (1993) has shown, in the context of the NMC MRF model (National Meteorological Center, USA; Medium Range Forecast), that the predictions show a rapid decrease in this ability to reproduce blocking during the first days of forecast, reaching a minimum around day ten. During the later stages of the forecast, the model recovers, drifting towards a more stable situation of higher (albeit still lower than observed) frequency of occurrence of blocking episodes. This can be considered the model's own blocking climatology. In other words, the model tends to miss blocks while drifting towards its own climatological equilibrium in the first days of forecast. This can be qualitatively understood by thinking that the process of drifting involves the use of transient modes by the model, reducing the incidence of blocking which is by definition a stationary or quasi-stationary phenomenon. Once the model has reached an equilibrium (as in long climate model integrations), blocking frequency recovers.

The literature contains a comparatively smaller number of papers dealing with blocking diagnostics in GCMs used for climate simulations. Recent examples of such works are Blackmon et al. (1986), Mullen (1986) and, in the context of the ECHAM3 model, Sausen et al. (1993) and May (1994). The present work also analyzes the outputs of ECHAM3 integrations in different configurations of resolution and of oceanic boundary conditions, and has the aim of constituting a conceptual tool for an extension of the work to all the models participating in the Atmospheric Model Intercomparison Project (AMIP, Gates 1992).

Two of the analyzed runs make use of prescribed observed sea surface temperatures (SSTs); these integrations are of particular interest in the light of previous works (Ferranti et al. 1994) that showed the influence of tropical variability (mainly SSTs) on extended range prediction. Such influence was given a possible explanation by Palmer (1989) and Palmer and Tibaldi (1988), which involved the dependence of large-scale instability of the forecast on the amplitude of the Pacific North American (PNA) mode. The same topic was also addressed by Ponater et al. (1994) in the context of a climate model.

In Sect. 2 the details of the analysis technique are explained, and in Sect. 3 some remarks are presented on the natural interannual variability of observed blocking. After introducing and analyzing longitudinal blocking frequency as simulated by the models in Sect. 4, a short discussion on the dependence of the blocking index response on the systematic error and on the mean state of the model is presented in Sect. 5. In Sects. 6, 7 and 8 the behaviour of the model in reproducing the statistical features of blocking is further assessed by comparing it to the observations. Some conclusions are presented in Sect. 9. The Appendix Figs. A1 and A2 show mean, low and high frequency standard deviations for the analysis and the different versions of the model. Together with the Systematic Error maps shown in Fig. 3, these figures constitute a reference background on the model's general behaviour.

2 Description of data sets, model and analysis procedure

The database used in this study consists of daily 500hPa geopotential height (GPH) fields at 12:00 GMT, both observed and produced by long integrations (several decades) of general circulation models.

Observed data have been obtained merging NMC analyses for the period December 1949 – December 1979 with ECMWF analyses for the subsequent period January 1980 – February 1992, forming a daily dataset of 42 years plus three months of an additional winter. The original NMC data consists of Northern Hemisphere fields on the NMC octagonal grid, while ECMWF data consists of global fields represented by spherical harmonics coefficients truncated at triangular truncation 40. All the data were reinterpolated on a regular latitude–longitude grid ($3.75° \times 3.75°$) and only regions north of 22.5 °N were considered.

Model data were mostly produced by integrating the ECHAM3 global model (ECmwf - HAMburg) at different horizontal resolutions and using different prescriptions of SST lower boundary data. ECHAM3 is the third generation global general circulation model developed at the Max-Planck-Institute für Meteorologie, Hamburg, Germany and at the University of Hamburg. Details about its formulation are contained in the model documentation (DKRZ 1993) and in Roeckner et al. (1992), which also contains basic diagnostic information on the model's climatology. Only a brief description of the model's main characteristics will be given here. In the Appendix Figs. A1 and A2 a summary of 500 hPa mean and high and low frequency standard deviations is shown for the period February–March. The reasons for the choice of this period are described later.

The prognostic variables of ECHAM3 include vorticity, divergence, temperature, water vapour, cloud water and surface pressure. The model equations are solved on 19 vertical levels in a hybrid sigma-pressure system by using the spectral transform method with triangular truncation at wave numbers 21 (T21) or 42 (T42). Non-linear terms and physical processes are, however, evaluated at grid points of a Gaussian grid providing a nominal resolution in latitude and longitude of 5.625° for T21 truncation and of 2.8125° for T42. A second-order horizontal diffusion scheme is applied to vorticity, divergence and temperature. The diffusion is limited, however, to the high wavenumber end of the resolved spectrum. The radiation scheme is based on a two-stream approximation of the

radiative transfer equations with six spectral intervals in the infrared and four in the solar spectrum (Hense et al., 1982). Gaseous absorption due to water vapour, carbon dioxide and ozone is taken into account as well as scattering and absorption due to aerosols and clouds. The cloud optical properties are parametrized in terms of the cloud liquid water content.

The parametrization of cumulus convection is based on the concept of the mass flux scheme of Tiedtke (1989) and comprises the effect of deep, shallow as well as mid level convection on the heat, water vapour and momentum budgets. Cumulus clouds are represented by a bulk model including the effect of entrainment and detrainment on the updraft and downdraft convective mass fluxes. Stratiform clouds are predicted *per se*, in accordance with a cloud water equation including sources and sinks due to condensation/evaporation and precipitation formation. The vertical turbulent transfer of momentum, heat, and water vapour is based upon the Monin-Obuchov similarity theory for the surface layer and eddy diffusivity approach above the surface layer.

The effect of orographically forced gravity waves on the momentum budget is parametrized on the basis of linear theory and dimensional considerations. Gravity wave drag parametrization, however, is not included in the T21 integrations. The land surface scheme (Dümenil and Todini 1992) considers the heat and water budgets in the soil, snow cover and land, and the heat budget of permanent land and sea ice. The heat transfer equation is solved in a five layer model assuming that the heat flux vanishes at the bottom-most layer. Vegetation affects such as interception of rain and snow in the canopy and the stomatal control of evopotranspiration are, however, currently grossly simplified in this scheme. The integration is performed following a semi-implicit scheme with leap-frog time filter, with the time step of 40 minutes at T21 truncation and 24 minutes at T42.

This work examines four integrations of the ECHAM3 model, at the two horizontal resolutions corresponding to T21 and T42 truncations and with two different specifications of the sea surface temperatures (SSTs): climatological or observed. The observed SSTs consist of individual monthly means in the period 1979–1988. SSTs during model integrations are however updated almost continuously, i.e. every model time step. Single time step SSTs are obtained by linear interpolation of observed monthly mean data, attributed to the central days of successive months. Observed SSTs integrations do not therefore contain any forcing expressing variability with time scales shorter than one month. The 1979–1988 period corresponds to the ten year period conventionally taken as a standard in the Atmospheric Model Intercomparison Project (AMIP, Gates 1992), in which the analyzed model participated. The climatological SSTs used are observed monthly means computed over the entire 1979–1988 period. The time interpolation procedure is identical to the one used in the case of observed SSTs, described already. The observed SSTs integrations are referred to as GAGO (Global Atmosphere Global Ocean) runs, while the climatological SST integrations are usually called "control runs".

Additionally, some results from a further ECHAM2 T21 control integration are considered. ECHAM2 (an older version of the ECHAM model) differs from ECHAM3 in the physical parametrization package and particularly in the moist convection scheme (Roeckner et al., 1992). A summary of the characteristics of all integrations considered in this work is shown in Table 1.

An objective blocking index, based on the TM modification of the original Lejenäs and Økland (1983) index will be used throughout this study. The nature of the index and the criteria used in its construction are extensively discussed in TM. Here only a brief definition is given.

The GPH gradients GHGS and GHGN are computed for each longitude:

$$\mathrm{GHGS} = \frac{Z(\phi_0) - Z(\phi_S)}{\phi_0 - \phi_S} \tag{2.1}$$

$$\mathrm{GHGN} = \frac{Z(\phi_n) - Z(\phi_0)}{\phi_n - \phi_0} \tag{2.2}$$

where:

$$\phi_n = 78.75\,^\circ\mathrm{N} + \Delta$$

$$\phi_0 = 60\,^\circ\mathrm{N} + \Delta \tag{2.3}$$

$$\phi = 41.25\,^\circ\mathrm{N} + \Delta$$

$$\Delta = -3.75^\circ, 0^\circ, 3.75^\circ$$

A given longitude is defined as blocked on a specific day if both following conditions are satisfied (for at least one value of Δ):

$$\mathrm{GHGS} > 0, \tag{2.4}$$

$$\mathrm{GHGN} < -10\ \mathrm{m/deg\ lat} \tag{2.5}$$

Similarly to TM, the two main sectors of the Northern Hemisphere that are particularly prone to blocking are

Table 1. Summary of the main characteristics of the model integrations analyzed

Model	Horizontal representation	SSTs	GWD	Length of integration
ECHAM2	T21	Climatological	No	20 y
ECHAM3	T21	Climatological	No	33 y
ECHAM3 GAGO	T21	Observed	No	10 y
ECHAM3	T42	Climatological	Yes	20 y
ECHAM3 GAGO	T42	Observed	Yes	10 y

then identified and defined, with the following longitudinal limits:

Euro-Atlantic: 26.25 °W – 41.25 °E
Pacific: 150 °E - 221.25 °W

A sector is then taken to be blocked if three or more adjacent longitudes within its longitudinal limits are blocked according to the local and instantaneous TM index definition.

These criteria are sufficient to define a local (in time and space) block-like pattern. True synoptic blocking (i.e. in the Rex sense) however requires a certain time-persistence of the event. Consequently, a further requirement has to be added to the sector blocking definition, which was arbitrarily chosen to reject any sector blocking lasting less than five days, again consistently with TM. A number of "threshold-edge events", which intermittently may or may not fulfil the requirements of the index were found, requiring special tapering of the time sequence. More details about the algorithm used in this case will be found in Sect. 4.

An index like the one presented here, based on the detection of local geostrophic easterly flow, has been shown in previous works (Lejenäs and Økland, 1983; TM; Tibaldi et al, 1994, 1995) to be satisfactorily consistent with the synoptic assessment of blocking events. Furthermore, since the main objective of this study is to perform a comparative analysis of observations and model outputs, the specific nature of the index should not affect the main conclusions, with the notable exception of the work reported in Sect. 5, on the effects of model systematic errors.

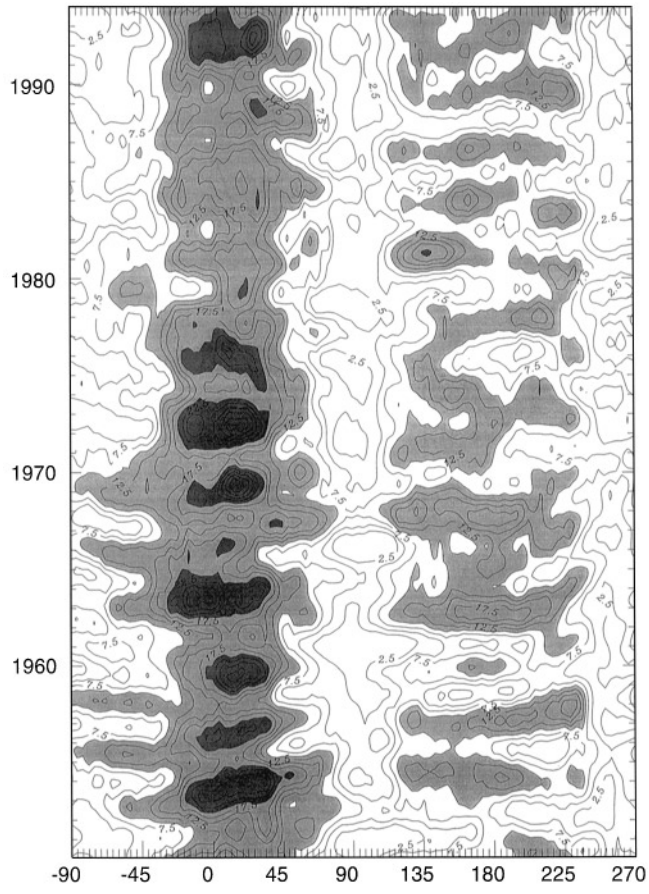

Fig. 1. Interannual Hovmöller diagram of monthly mean blocking frequency, low-pass spectral filtered in time with a cut-off period of 2.5 y. Areas higher than 10% and 20% are *shaded*. Longitude is on the x-axis and time in years is on the y-axis

3 Observed interannual variability of blocking

It is not in the scope of this study to describe the observed features of blocking. In TM and Tibaldi et al. (1995) discussion on the observed blocking is carried out extensively, using the same index as in the present study. Nevertheless, it is of some importance to point out here an important characteristic of the statistics of blocking climatology that is not addressed in the quoted works, i.e., the interannual variability. For this reason, Fig. 1 is presented which shows the isolines of observed blocking frequency as a function of time (one value per month) and longitude (a Hovmöller diagram).

The diagram refers to the observed period 1950–1993 and was obtained by (low-pass) spectrally filtering out all time-variability with periods shorter than 2.5 y. There are a number of considerations that can be made from this diagram; first of all, it can be seen that very large variations are evident within time spans of very few years. Moreover, the pattern, observed at fixed longitudes, seems to show evidence of some quasi-periodicity or intermittency. This variability is also evident on longer time scales, such as the one defined by the comparatively low activity period of the 1980–1990 decade in the Euro-Atlantic region.

An interpretation of this variability (let alone an explanation!) is beyond the scope of this work and this figure is reported here only to illustrate the sensitivity of the observed blocking statistics on the sampling period. The integrations analyzed here, in fact, make use of prescribed SSTs referring exactly to the decade of lower activity. On the other hand, ten years appear to be a period just long enough to smooth out at least the (relatively) higher-frequency variability (around four–five years) associated with the maxima of blocking activity, particularly evident in the 1950–1978 period and almost absent in the 1979–1990 period.

4 Blocking frequencies

In Fig. 2 blocking frequency diagrams as a function of longitude are shown for observed and simulated winters (DJF). These diagrams reflect the behaviour of the instantaneous (daily) and local (in longitude) blocking index as defined by equations 2.1–2.5 above. Since no time-duration constraint was added, we are actually computing the frequency of occurrence of "blocking-like patterns" rather then actual synoptic blocking episodes, in the sense of Rex (1950a, b). The blocking frequency as obtained from the observed data (dashed line) is shown for reference in each panel. The entire dataset of 43 winters has been used for

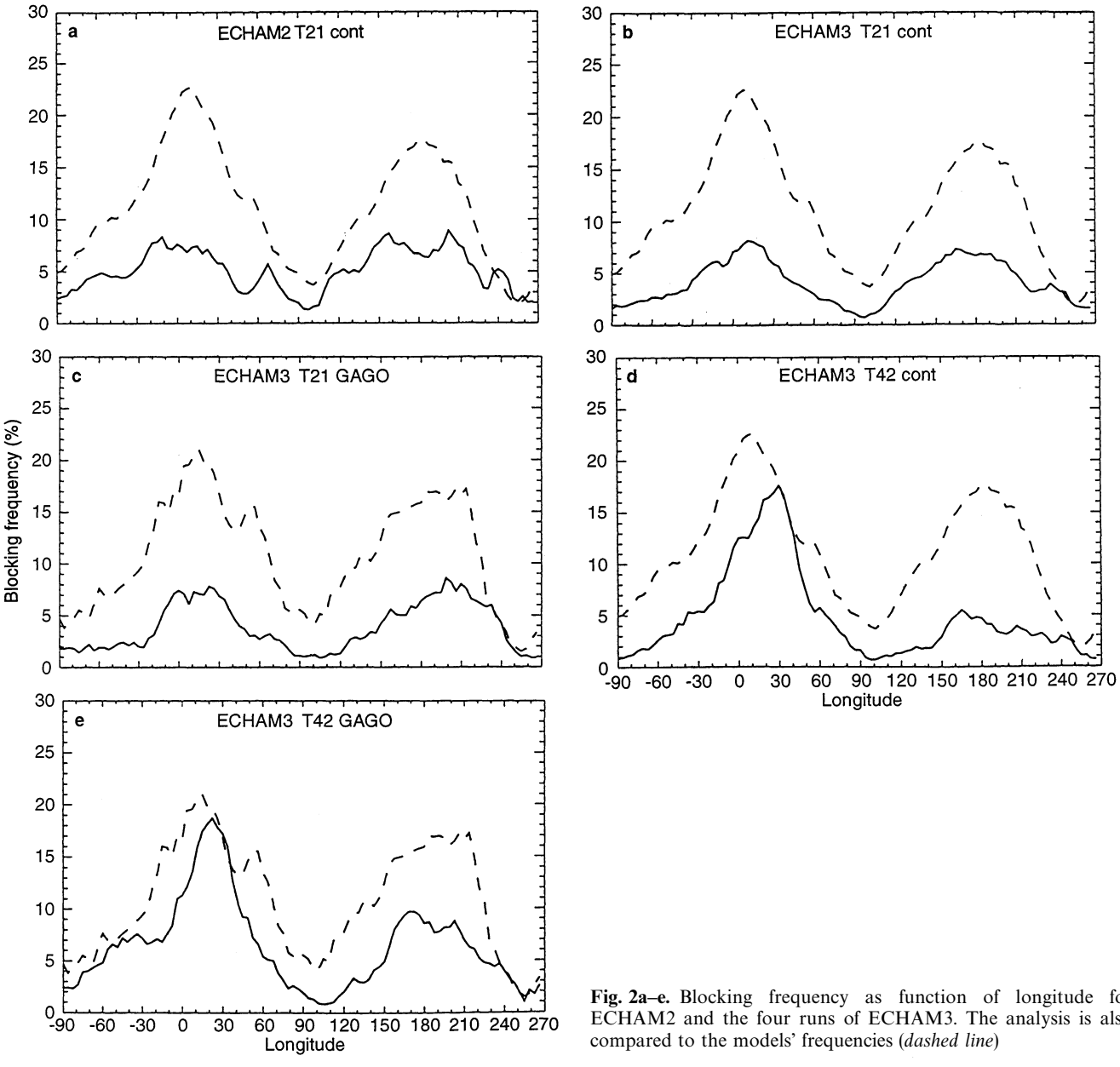

Fig. 2a–e. Blocking frequency as function of longitude for ECHAM2 and the four runs of ECHAM3. The analysis is also compared to the models' frequencies (*dashed line*)

comparison with the control integrations, while only the 9 full winters contained in the AMIP period 1979–1988 have been used to assess the GAGO runs.

Both observed blocking frequencies (dashed in each panel) show the well-known blocking maxima in the Euro-Atlantic (hereafter E-A) and Pacific (PAC) sectors. A third secondary peak, corresponding to the Ural blocking, is also visible at around 60 °E, more clearly in the AMIP period alone.

Figure 2a shows the output of ECHAM2, of which only a control run was available. In this panel the separation between the two sectors is visible but the amplitude of the simulated frequency is much lower than observed.

Moving to Fig. b and c (i.e. considering ECHAM3 T21, the next generation ECHAM model, with different, supposedly better, physics), no particular improvement of the simulation of the blocking frequency is observed, neither in the control (Fig. 2b) nor in the GAGO (Fig. 2c) run. Conversely, an improvement is observed with further movement to the higher resolution ECHAM3 T42 model. The improvement involves only the E-A sector in the control run (Fig. 2d), but both sectors in the GAGO run (Fig. 2e). In this last integration the best ever performance of any version of the ECHAM model as far as Pacific blocking is concerned can be observed.

Moving from ECHAM2 to ECHAM3 there appears to be no measurable improvement in modelling blocking unless the improvement in physical parametrizations is accompanied by an increase in horizontal resolution. Unfortunately, the fact that a T42 integration of ECHAM2 is

not available does not allow us to assess more accurately the importance of physical parametrizations against resolution in bringing about the observed improvement. A complete "cross comparison" of the two models is not possible: however, what can be said is that in this case the potential improvement due to the change in the physical parametrization cannot be realized without a sufficiently high model resolution.

A second consideration concerns the different sensitivity of the two blocking sectors to a change in the lower boundary SSTs. An increase of model resolution appears to be sufficient to improve the simulation of blocking in the E-A sector, while the presence of a more realistic variability in the oceanic lower boundary condition seems to be necessary, in addition to the higher resolution, to enhance the simulation also in the PAC sector. This suggests the hypothesis that the two blockings may be the product of at least partially different dynamical processes, the E-A being more reminiscent of nonlinear internal dynamics, while the PAC appearing to be more influenced by the interaction with the sea surface. It is interesting to remark that sensitivity of Pacific blocking to tropical SST anomalies is also shown by Ferranti et al. (1994). In this work, four winter T63 integrations of the ECMWF model are performed with the climatological SSTs modified by an artificially superimposed anomaly. The presence of a warm anomaly in the Indonesian Archipelago is found to trigger a strong enhancement of blocking frequency in the Pacific sector, and only a much smaller increase in the Euro-Atlantic. It must also be noted that the low-frequency variability (LFV) map of the ECHAM3 T42 GAGO integration (Fig. A2i) shows in the Pacific area an overestimation of the maximum of variability; this maximum is however somewhat shifted northward, towards a region that is partially out of the area of synoptic midlatitude blocking (also compare with the analysis, figure A2g). This overestimation represents an exception to the general behaviour of GCMs of comparable horizontal resolution which usually tend to underestimate variabilities. An ideal experimental framework for testing blocking sensitivity to SST variability, on time scales shorter than one month could be made with coupled models.

ECHAM3 T42 has been also analyzed in Sausen et al. (1993). In their work, blocking frequency show a less severe underestimation of the Pacific blocking, that is nevertheless accompanied by an evident latitudinal displacement of the maximum. This result is consequently in substantial accord with the present study, considering that the index used here works at an almost fixed latitude.

5 Systematic error and blocking index

At this point it may be wise to consider the possible interactions between the nature of the blocking index chosen and the systematic error (SE) of the models. Since the index is defined on the complete field of the 500 hPa geopotential height, it is not unreasonable to think that, if the model is affected by systematic errors, these might in turn affect adversely the applicability of the objective blocking index to the model fields. It would then be difficult to take this interaction into account in evaluating subjectively the output of different versions of the model, affected by different SEs. In this section, the influence of systematic error will then be singled out by subtracting it from the daily fields to which the blocking index is applied: first zonally averaged error and then the full systematic error of the 500 hPa GPH will be subtracted.

Before performing the analysis, systematic errors maps will be presented. In Fig. 3 the systematic error is shown for the four ECHAM3 integrations in the usual winter season (December, January and February, DJF). The SE is defined as the difference between the mean 500hPa GPH fields of the models and that of the observations. Control runs are compared with the mean computed using all the available observed data, while for GAGO runs only the period 1979–1988 has been used. The DJF SE of both T42 models shows a larger amplitude with respect to the lower resolution models. The T42 integrations also show a tendency to zonalization which is not evident at T21.

This increase of SE amplitude and of zonalization with model resolution is a well-known phenomenon in the context of NWP and has been reported by e.g. Tibaldi et al. (1991) for the ECMWF extended range forecast model, by Boyle (1992) in the context of climate simulations with the same model, and more generally by WMO (1991). This problem has partially been explained in terms of an erroneous balance between the convergence of momentum flux taking place in mid-troposphere midlatitudes and the efficiency of the processes resulting in momentum sink, due to mountains and surface friction (Palmer et al. 1986; Miller et al. 1989).

In higher resolution models, horizontal convergence of mid-tropospheric westerly eddy momentum flux and the associated rectification process are better resolved, while the vertical downward transport of momentum and the coupling with the surface often remain inadequate. The presence of the gravity wave drag (GWD) parametrization alone is often insufficient in balancing the zonalization due to the flux of eddy momentum. This can also account to a certain extent as to why the zonalization, present even with GWD parametrization, is particularly large in the Pacific; the GWD parametrization acts locally, and does not include the longitudinal and latitudinal displacement of waves and is triggered by the presence of orography (Palmer et al. 1986). In lower resolution models, on the contrary, lower-than-observed mountain drag and lower-than-observed westerly momentum flux convergence tend to balance and to establish a compensating error situation.

Given the zonal character of the SE, and given that the blocking index is in fact an index of the local zonality of the flow, it becomes important to single out the dependency of the index response on the SE. The DJF SEs also tend to show relative maxima in correspondence to the sectors of the Northern Hemisphere where blocking is more frequent. These maxima are nevertheless less pronounced than in NWP models of comparable resolution, where SEs often have the shape of a reverse blocking pattern (see e.g. Tibaldi et al. 1994). The fact

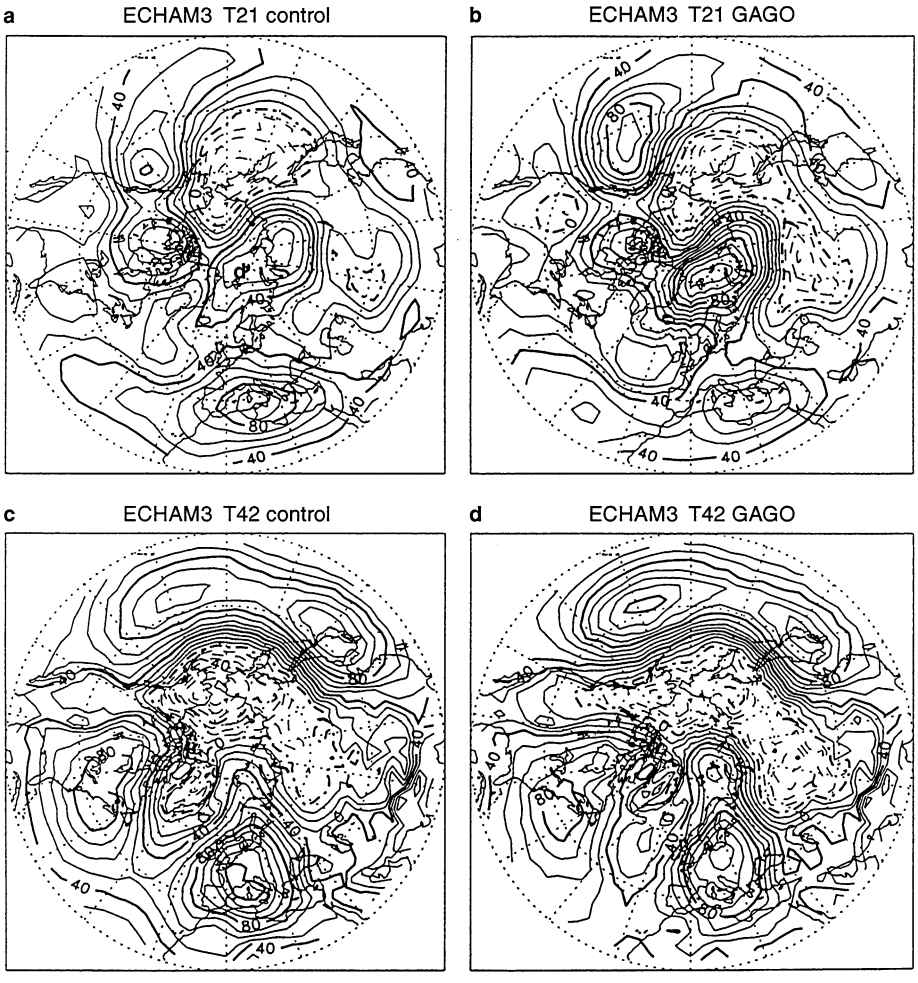

Fig. 3a-d. 500 hPa GPH systematic error as a difference of the models' and the observational mean field for DJF. **a** is ECHAM3 T21 control run, **b** ECHAM3 T21 GAGO, **c** ECHAM3 T42 control, and **d** ECHAM3 T42 GAGO

that in climate models SEs appear to be somewhat less clearly related to blocking should not be too surprising, in the light of the discussion in the introductory section.

In Fig. 4 blocking frequencies (analogously to Fig. 2) are shown for the modified output of the two climatological SSTs integrations in DJF. The systematic error of every month was computed and assigned to its central day. A daily SE for the whole year was then built by linearly interpolating between the two central days of adjacent months. From every single daily model output was then subtracted the corresponding systematic error, obtaining a "corrected" dataset. Another alternative dataset was obtained by subtracting from every model output only the zonal mean of the systematic error, obtaining a "zonally corrected" dataset. This allows us to compare the response of the index to the zonalizing SE.

In the right column of Fig. 4 (b, d and f), it can be seen that considerable effects of the SEs corrections are found on the T42 version of ECHAM3; this is most likely due to the above mentioned larger SE amplitude in the higher resolution integrations. The subtraction of the full systematic error causes a considerable enhancement of the blocking frequency, this enhancement being quite strong for the PAC sector but much smaller for the E-A. This effect can be understood by comparing Fig. 4 with Fig. 3c. In the T42 control run SE, a strong area of zonalization is found in the Pacific, exactly at the latitude relevant for the blocking index. Removing such strong zonalization therefore causes therefore an enhancement in the index response.

Limiting the correction of the T42 to the zonal mean only (Fig. 4d) has a different effect on the two blocking sectors. The PAC only slightly increases in blocking frequency, while the E-A becomes overestimated. The process of longitudinal averaging in the E-A sector leads to an excessive response; while on the PAC sector it reduces the correction of the zonalizing error, in the T21 integration on the contrary, only a small improvement is observed after the subtraction of the full SE, while the zonal-only correction is almost negligible. This is in line with the fact that the T21 integrations have negligible zonalization problems (see earlier).

From this consideration, we can conclude that in the E-A sector the influence of the systematic error on the index response is negligible, and that this adds confidence to all diagnostic results obtained in this sector. The case of the PAC sector is less clear, since the enhancement due to the removal of the zonalization is marked. Having said

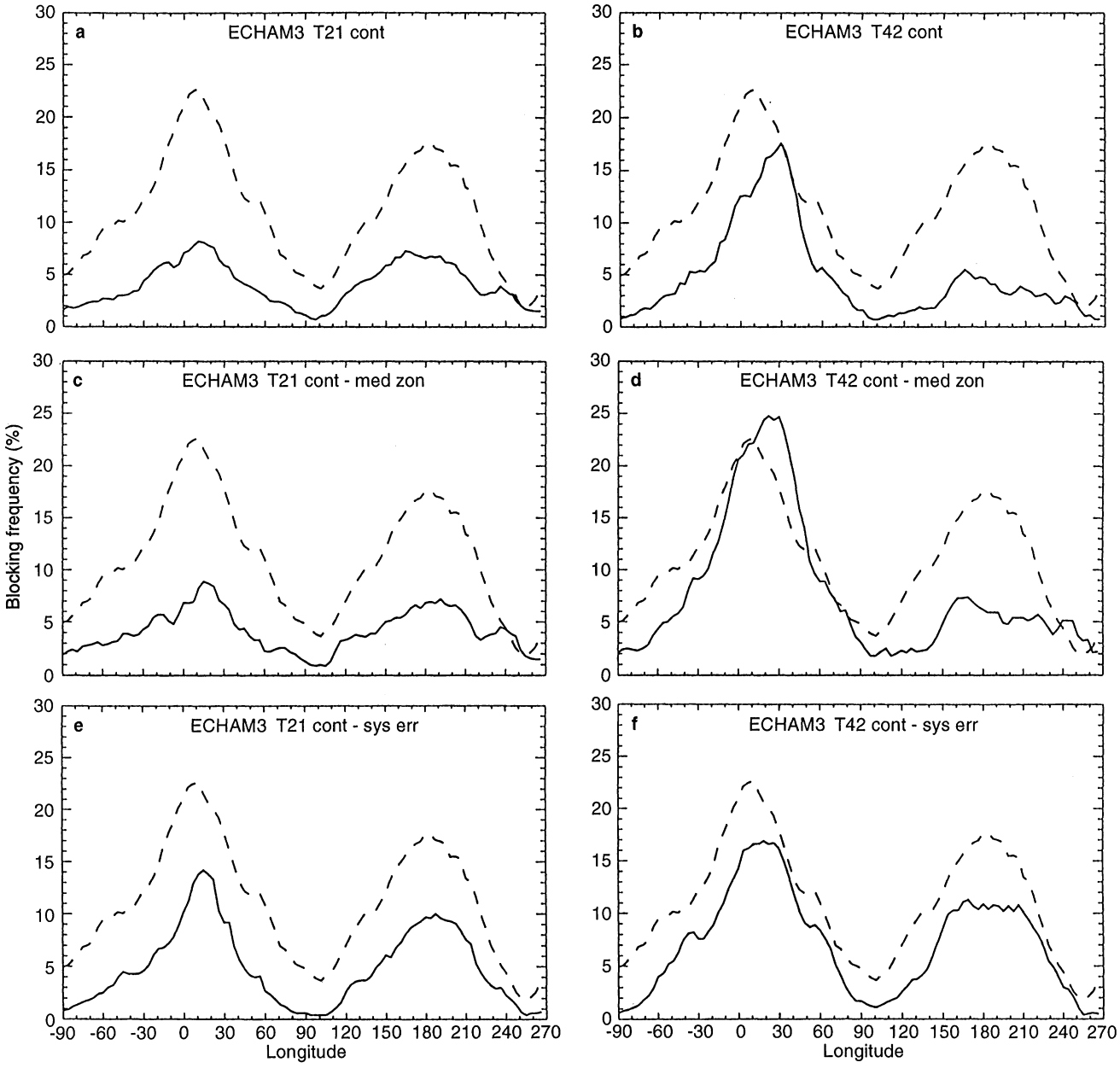

Fig. 4a-f. Blocking frequency as a function of longitude for the corrected output of ECHAM3 T21 and T42 control runs. **a** and **b** are the same as Fig. 2**b** and **d** respectively. **c** and **d** are computed from the outputs of the two integrations after subtraction of the zonal mean of the systematic error. **e** and **f** are computed after the subtraction of the complete field of the systematic error.

this however, it must be pointed out that it is impossible to disentangle blocking and the mean flow completely, since the occurrence of the former strongly contributes to the formation of the latter. This problem can be partly addressed by constructing a blocking index which is completely independent from the zonal part of the flow. Such indices, based only on eddy fields, reveal however low synoptic efficacy, although some improvements have recently been attained (Kaas and Branstator 1993). As far as this analysis is concerned, the conclusion is that, as opposed to the conclusions for the E-A sector, the results for the PAC sector should be considered with some extra caution, since the possibility exists that the index might slightly underestimate the blocking frequency in models with large zonal systematic errors.

6 Seasonal cycle of blocking activity

In order to diagnose the seasonal cycle of blocking frequency both in models and in observations, it is important to distinguish between instantaneous blocking-like structures and actual synoptic blocking episodes; a further constraint on time duration must therefore be added to

the definition of the index. This further time-continuity constraint consists essentially in eliminating all blocking "episodes" (sequences of blocked days) shorter than five days. The application of this constraint is best performed after the elimination of the noise caused by one-day threshold-edge events (both positive and negative). The detailed criterion to create a directory of synoptically blocked episodes consists of the following two steps applied in sequence:

1. When two successive days are considered blocked by the index in a sector and are followed by a non-blocked day and then by two more successive blocked days, the whole event is considered as a five day long block, assuming the "hole" simply as an index failure. An analogous "tapering" criterion is applied in the cases of a single non-blocked day preceded (followed) by three blocked days and followed (preceded) by a single blocked day.

2. All episodes of blocking shorter than five days are then excluded from subsequent analysis.

As mentioned before, the first step consists of a "cleanup" of the dataset from short threshold-edge events, while the second step is a requirement of time duration. Time duration is in fact one of the main characteristic of synoptic blocking, also in the classical definition given by Rex (1950a, b) in the literature. The choice of five days as the limit is arbitrary and stems from the compromise between having sufficiently long blocks and a sufficiently large statistical sample of episodes. After the application of this further constraint, it is possible to produce diagrams similar to Figs. 5 and 6, where the annual cycle of blocking

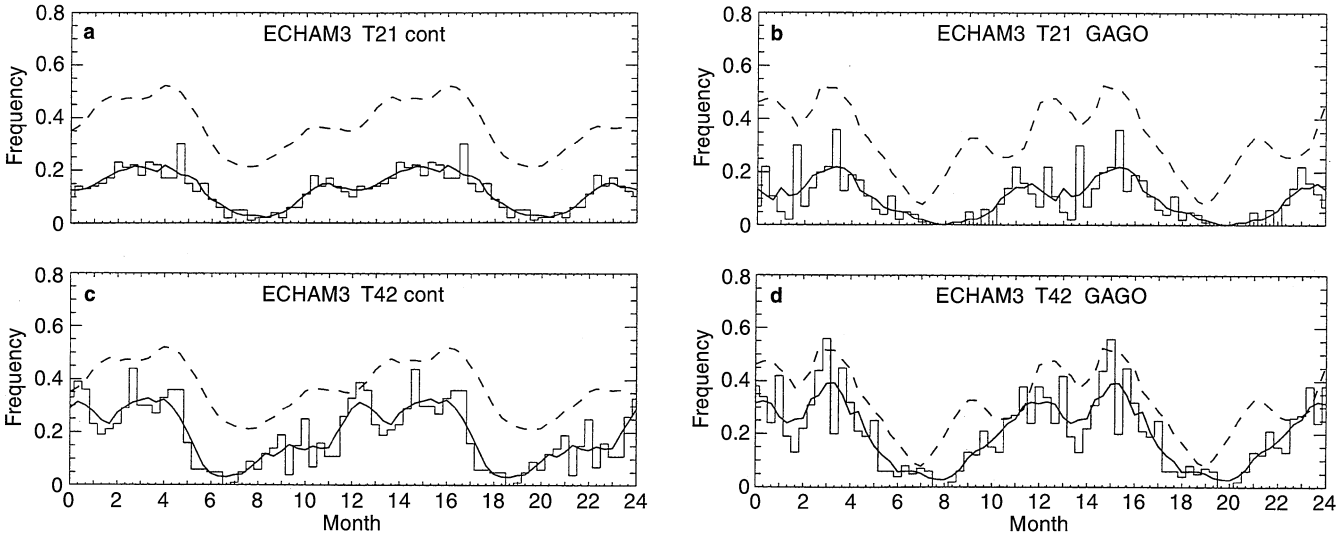

Fig. 5a–d. Annual cycle of sector blocking frequency as average number of blocked days per decade. *Smooth line* is a polynomial interpolation. Analysis is superimposed (*dashed line*). Euro-Atlantic sector. **a** ECHAM3 T21 control run, **b** ECHAM3 T21 GAGO, **c** ECHAM3 T42 control run, and **d** ECHAM3 T42 GAGO

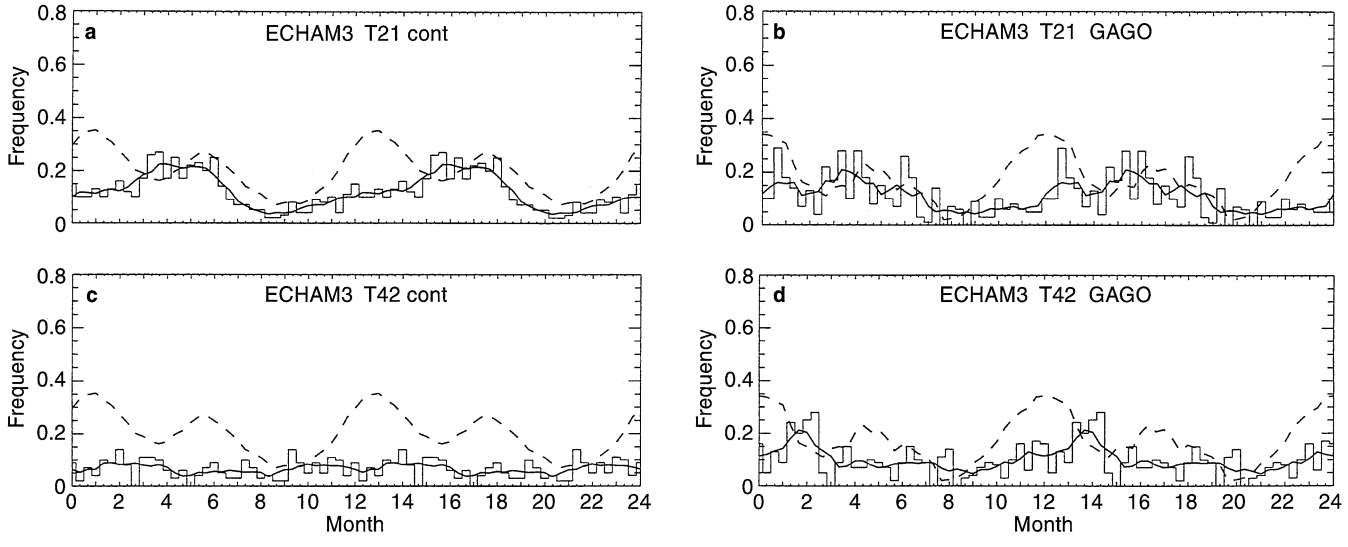

Fig. 6a–d. As in Fig. 5 but for the Pacific sector

frequency in the two blocking sectors, obtained by computing the average frequency of blocked days for each ten day period of the month, is shown (the observed cycle is dashed). The annual cycle is repeated twice along the x-axis, to show evidence of the periodicity more clearly.

As can be seen, the two sectors are characterized by different seasonal cycles. With the help of these diagrams, it can be seen that blocking is not particularly a winter phenomenon in the E-A sector (although most of the literature mainly concentrates on that season), rather that the yearly maximum takes place in spring. The PAC sector on the contrary shows a more convincing winter maximum. For this reason, in the remainder of this work when the need arises to concentrate on a single season, the period February–March (FM) will be chosen as the reference period for the E-A sector. This choice has the advantage of isolating a relatively sharp seasonal peak, but also of considering a period not too different from the winter season on which much of the available literature is concentrated. Additionally, for the AMIP period alone, the FM period for the E-A sector shows the highest peak as well. On the other hand, for the Pacific, the period considered will still be the usual DJF.

Figures 5 and 6 show the annual cycles of sector blocking activity as simulated by ECHAM3 in the different configurations compared to observation (dashed line). As usual, the GAGO runs are compared to the observations relative to the period 1979–1988. In the E-A sector, ECHAM3 T21, both control and GAGO, shows the capability to reproduce the shape of the annual cycle, although with a much reduced amplitude. The lower amplitude could be expected from the similar behaviour of the longitudinal blocking frequencies diagrams earlier (Fig. 2). The T42 version maintains the same ability to reproduce the shape of the seasonal cycle, but in addition has a more realistic amplitude.

The ECHAM3 T42 control run shows a shift in time, compared to observations. In the E-A the shift corresponds to the model being approximately one month "too early" in simulating minima and maxima. In Fig. 5c and d, show an enhancement of amplitude in moving from the control to the GAGO integration. This behaviour has already been observed in Fig. 2, although it can now be seen that this improvement involves only the DJF period and not other seasons. Contrarily to the E-A, in the PAC sector it is not possible to detect a time-shift with any confidence. On the other hand, a feature common to all models in the PAC is the generally poor performance in winter.

7 Blocking signatures

Figures 7 and 8 illustrate the "blocking signature" patterns, obtained by subtracting the composite field of all non-blocked days from the composite field of all blocked days (according to the index, but including the 5-day minimum time duration requirement) separately in the two sectors. These maps show shape, extension and intensity of the mean blocking structure both in the observations and in the models. They can also be regarded as the mean synoptic structures of the "regimes", as they are recognized by the index. Figure 7 refers to the FM period and to the Euro-Atlantic sector, while Fig. 8 refers to the DJF period during which the most intense maximum in blocking frequency is to be found for the Pacific sector (see Sect. 6). It can be observed in Fig. 7 that in all model integrations the position of the blocking high maximum is well placed. The comparatively weaker associated lows appear to be shifted to the west and to be weaker than observed, the westward shift being slightly less evident in the higher resolution integrations.

Concentrating for the moment on observed data alone (Figs. 7 and 8a), it may be noticed that blocking in both sectors is characterized by a neat and localized signature, with very little evidence of structures spatially remote from the quadrant under attention. A small exception is constituted by a weak cyclonic area immediately to the east of the blocking anticyclone, well separated from the large amplitude blocking low to the south of it. This feature is visible in both sectors, but it appears to be of somewhat larger spatial extent in the Pacific blocking case.

If the analysis is restricted to the ten year AMIP period alone (Figs. 7 and 8b), it becomes evident that such a short sample (the number of blocked days on the total number of days is reported in the lower-left corner of each panel) becomes insufficient to isolate neatly the blocking signatures in the two quadrants. This points towards a limit in the usefulness of "phenomena diagnostics" (Gates 1991) in evaluating model integrations of the order of ten years, when the atmospheric processes under study exhibit measurable natural variability on comparable time scales, as already mentioned in Sect. 3.

Turning our attention to model performance, it is evident that model behaviour is different in the two sectors and that it appears to be even more affected by sampling problems than for the real atmosphere. It is therefore reasonable to concentrate mainly on control runs (Figs. 7 and 8c, e). The main problem of models, representation of sector blocking patterns is connected with their inability to produce localized signatures. Additional weaker patterns appear, which in some cases (e.g. T42 control run, PAC sector) are reminiscent of well-known teleconnection patterns, e.g. a combination of PNA and NAO (North Atlantic Oscillation).

Another model feature worth pointing out, also typical of the T42 control run alone, is the erroneous longitudinal elongation of the blocking high in the PAC sector, which could also be interpreted in terms similar to those just outlined. A similar behaviour is not nearly as evident for the E-A sector and it is tempting to interpret this in terms of the differences in spatial extension between PNA and NAO, the latter being a more localized pattern resembling, in the right phase, an Atlantic blocking signature (Corti et al. 1997). These consideration, though, should be considered with caution due to the generally poor simulation of blocking in that sector.

8 Lifetime of blocking episodes

Figures 9 and 10 show the distributions of lifetime of blocking episodes for episodes longer than five days, in the

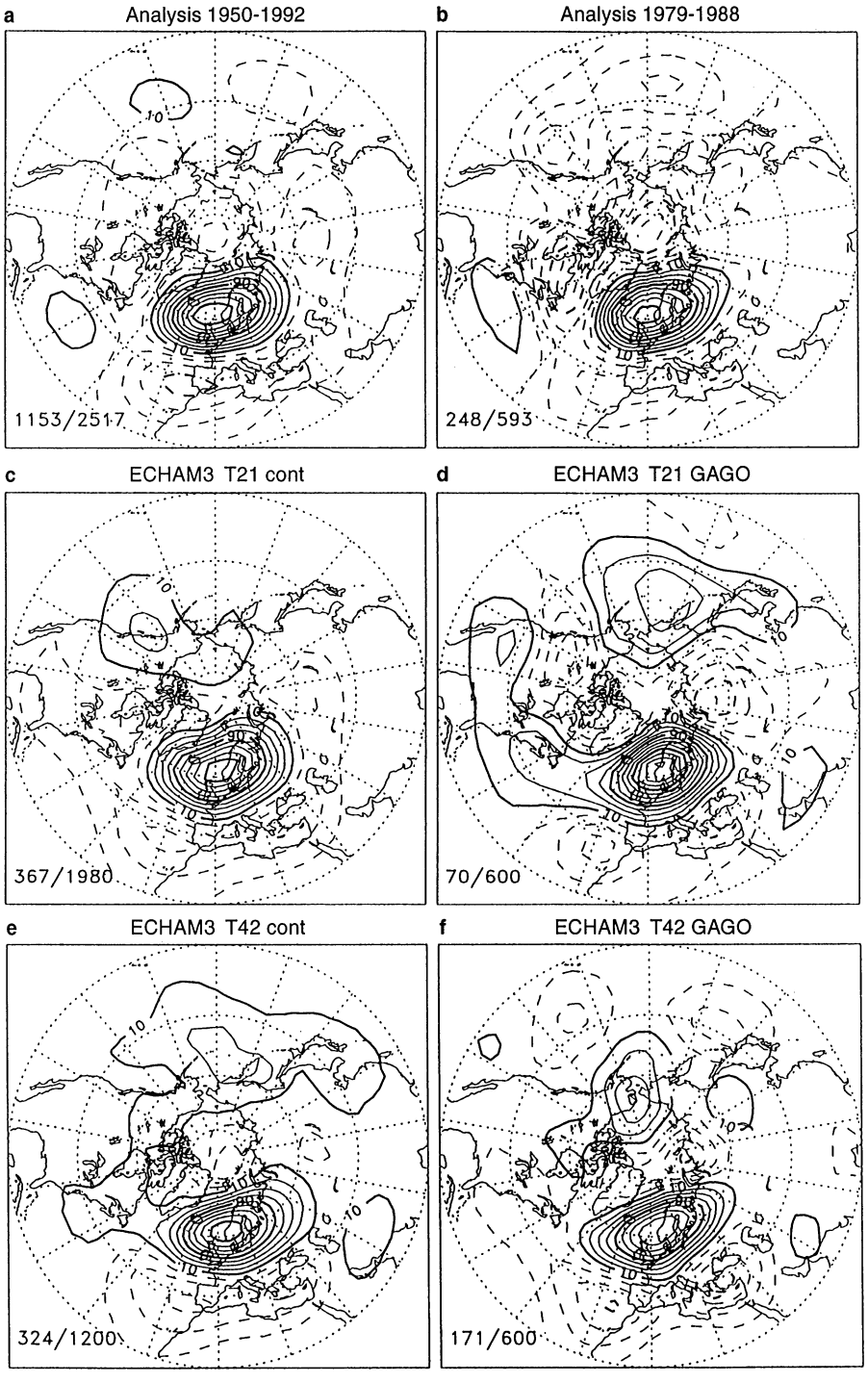

Fig. 7a–f. "Blocking signature" (i.e. the difference of blocked and zonal climate) of the Euro-Atlantic blocking in the February–March period. Contour interval 20 m. The *numbers* in the left corner refer to the fraction of days considered blocked by the index over the total number of days

observed data (black bars) and in the models (grey bars). The coloured bars (grey or black) represent the area between the mean value plus and minus the statistical uncertainty of each bin. Since the population of each bin is assumed to be Poissonian, the bar is given an error of square root of n, where n is the mean value of the bin. What can be seen is that in the Euro-Atlantic sector the T21 tends to produce a distribution of blocking length that is shifted towards the left side of the x-axis, (i.e. to the shorter duration end) while the T42 suffers less of this problem. In the Pacific sector, this seems no longer to be the case, the performances of the T21 being comparable to those of the T42. Also, the use of observed SSTs rather than climatology does not seem to influence appreciably model blocking lifetimes.

A diagram partially analogous to those of Figs. 9 and 10, although obtained with a radically different blocking index, is contained in Sausen et al. (1993), showing an exponential decrease in the blocking length distribution on the ECHAM3 T42 control run. The exponential

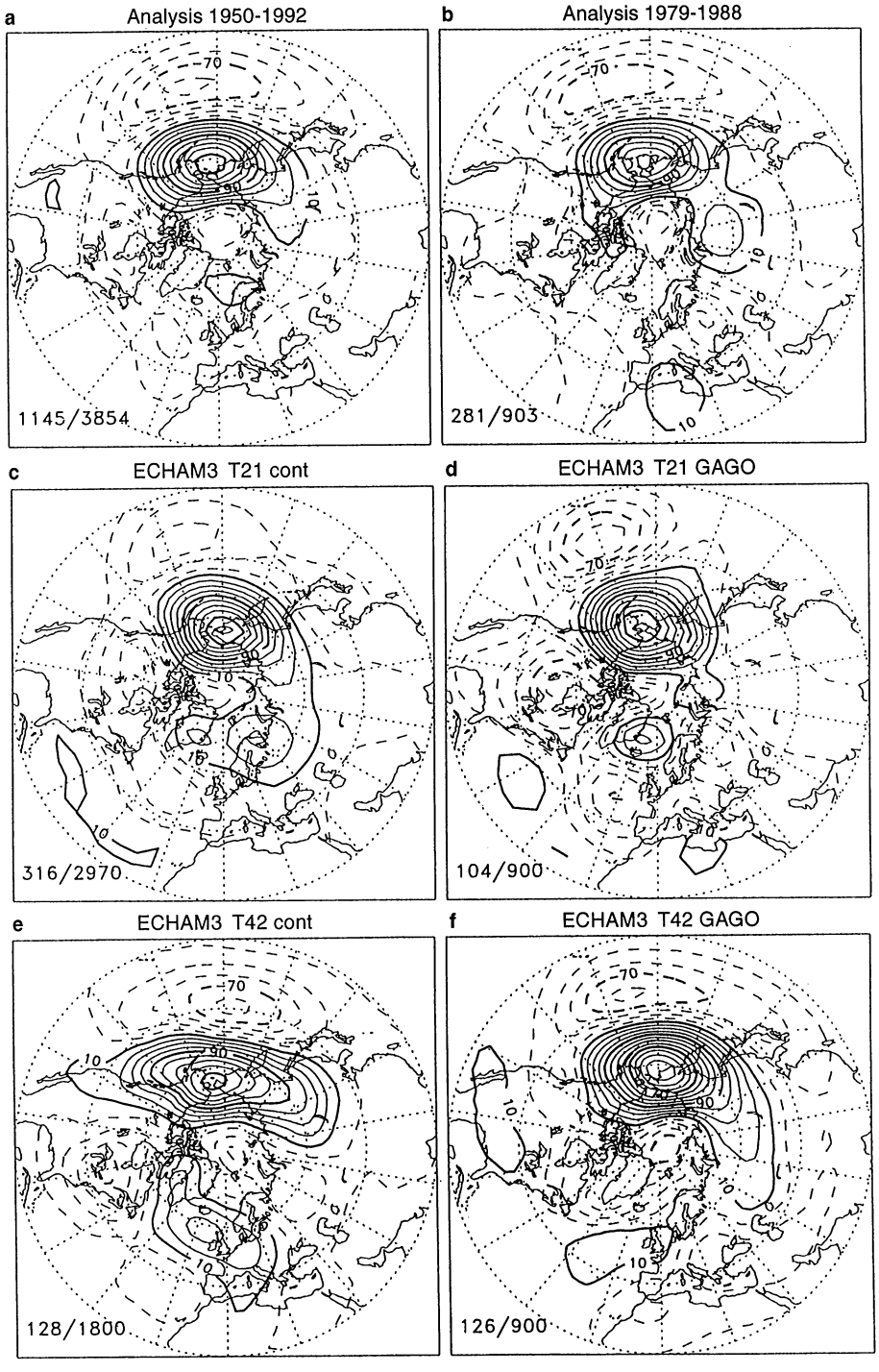

Fig. 8a–f. As in Fig. 7 for the Pacific blocking in the DJF period

decrease of blocking duration distribution was also found by Dole and Gordon (1983) on observed data and is usually interpreted as evidence of the independency of the probability of ending a blocking episode on its current duration.

An attempt to interpret this model behaviour (the bias towards shorter blocks) involves the mechanism of transient eddy forcing, firstly applied to blocking studies by Green (1977) and later developed in a number of work, e.g. Shutts (1983), Hoskins et al. (1983) and Mak (1990). The phenomenon was also documented in observational works (e.g. Austin 1980; Illari and Marshall 1983; Shutts 1986), mostly referring to Atlantic blocking. Due to its low resolution, the T21 model is unable to resolve baroclinic eddies adequately, and as their effect seems to intervene especially in blocking maintenance processes, this lack of baroclinic eddy forcing may be the cause of the simulation of a larger number amount of short-lived blocks than observed. The T42, on the other hand, can better resolve at least the larger

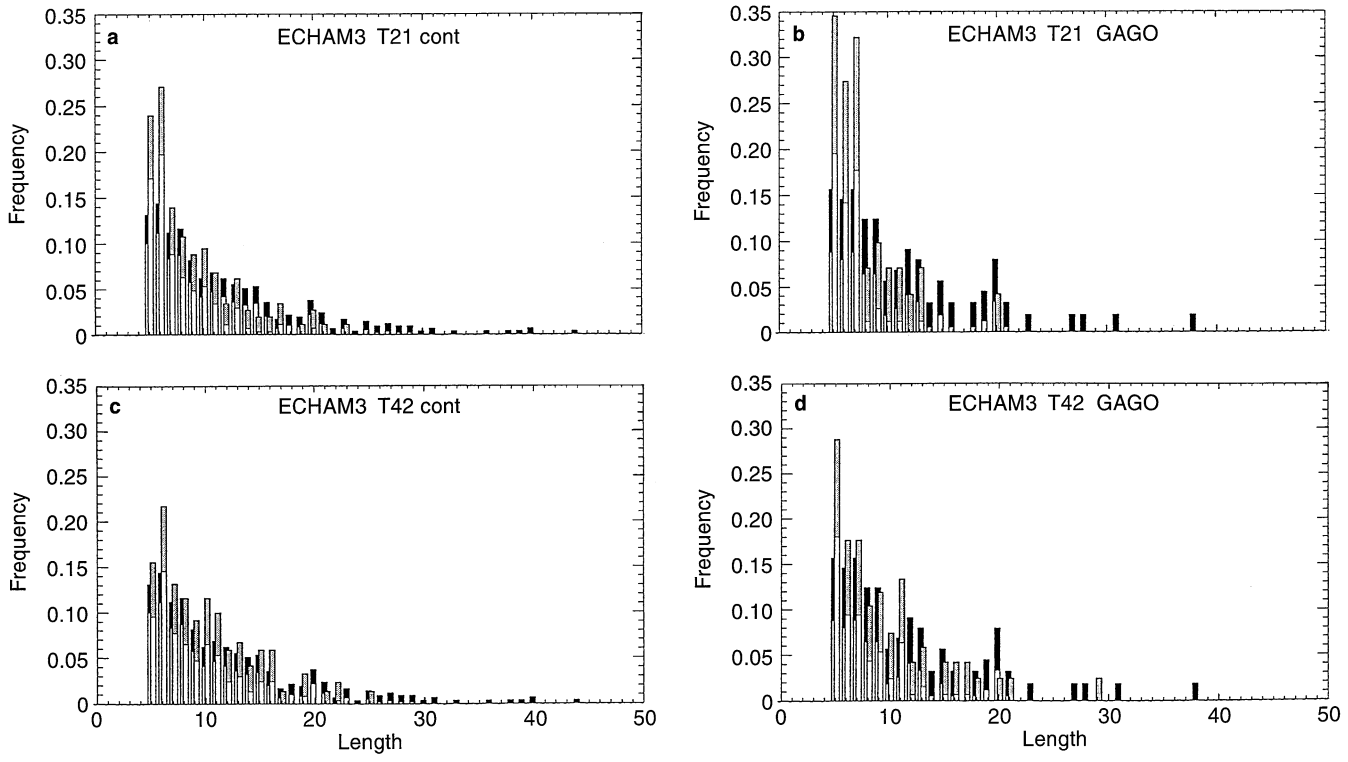

Fig. 9a–d. Frequency distribution of blocking length for the models' output in the Euro-Atlantic sector (*in grey*). Analysis is in *black*. The distributions are plotted with their statistical uncertainties, the areas in *colour* being the region enclosed between the mean value plus the statistical error and the mean value minus the statistical error

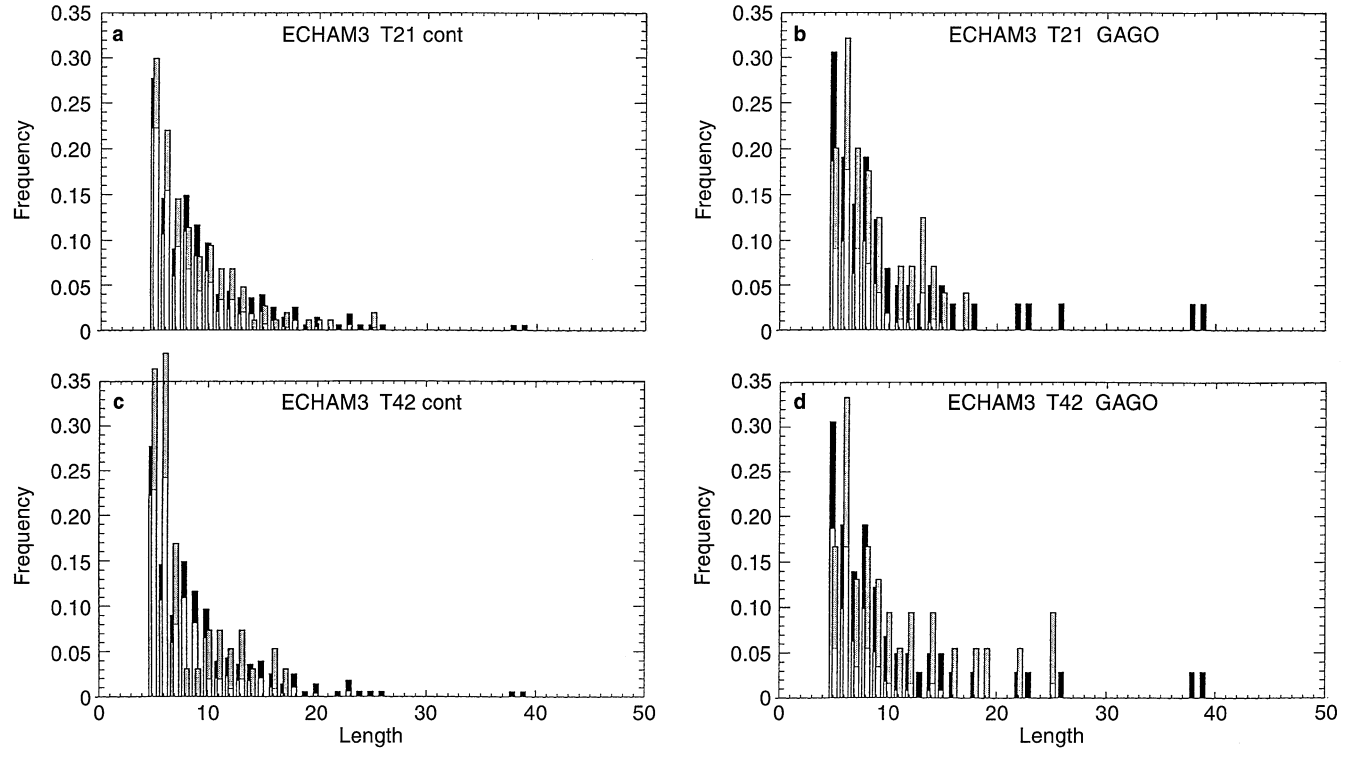

Fig. 10a–d. As in Fig. 9 but for the Pacific sector

scale baroclinic waves, and could therefore be less affected by this problem.

This last consideration may be suggestive of possible dynamical differences between the two sector blockings, hints and traces of which (both theoretical and observational) are found scattered in a number of papers, including this one. Eddy forcing is a process usually called upon in order to justify Euro-Atlantic blocking maintenance, while Pacific blocking is more often considered to be the product of either in-phase planetary scale waves superposition or linear/nonlinear resonance. The fact that the T21 integrations do not show the tendency to produce shorter than observed blocks in the Pacific sector is therefore consistent with this line of thought.

In a large set of extended integrations of the NMC medium range forecast model, Anderson (1993) noticed that the model distribution of frequency of blocking duration was biased towards longer blocks than in observations. The computations were made using an objective blocking index developed by the author. In this aspect ECHAM3 and NMC MRF seem therefore to show different behaviours.

Figure 11 shows two examples of the distribution of "non-blocking" length frequency. These diagrams represent the expectation time frequency between two successive blocking events. Only results from the ECHAM3 T42 control run are shown for the two sectors, superimposed on the observations. It can be seen that the expectation time frequency has an almost flat distribution, both for model and for observations. This can be interpreted as a consequence of the fact that the situation of "non-blocking" cannot be regarded as a physical phenomenon. On the contrary, blocking is indeed a physical-dynamical process, characterized by a local occurrence frequency, an onset, an average lifetime (a probability of decay) and an end. In other words, there is no dynamical symmetry between the "blocked state" and the "non blocked" or "zonal state".

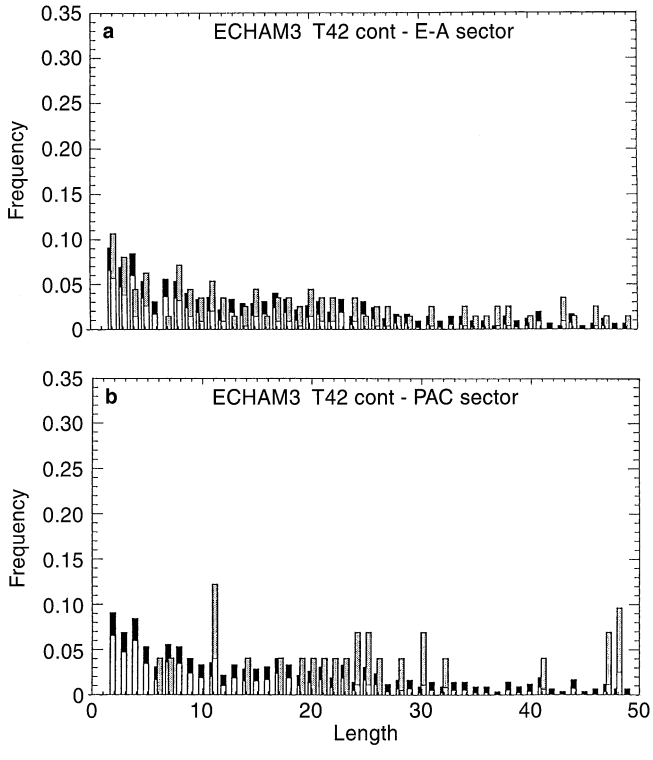

Fig. 11a,b. Examples of frequency distribution of non-blocking length (expectation time). ECHAM3 T42 control run is in *grey*, analysis in *black*. **a** is Euro Atlantic sector, **b** Pacific sector

9 Discussion and conclusion

The main purpose of this work was to assess the ability of the ECHAM GCM to represent atmospheric blocking when integrated for climate simulation purposes. This has been done by employing an objective blocking index to compute blocking frequencies and characteristics both in model output and in observed data. The model integrations considered, at different horizontal resolutions (T21 and T42) and with different versions of model physics (ECHAM2 and ECHAM3), used either climatological (control runs) or observed sea surface temperatures (so-called GAGO runs).

A general point that emerges from the work is the need for long enough datasets when analyzing blocking and generally low-frequency variability of models. This concern involves, in the present work, notably the GAGO integration, and should in this light be extended to the whole of the models participating in the AMIP project.

A number of considerations can be made about models' performance in simulating blocking. First of all, model performance appears to improve with the combination of increasing horizontal resolution (from T21 to T42) and switching to an improved set of physical parametrizations (from ECHAM2 to ECHAM3). Unfortunately, it is not possible to partition precisely the importance of the former against the latter in bringing about such an improvement.

Secondly, while an increase of model resolution is sufficient to improve the simulation of blocking in the E-A sector, the presence of a more realistic variability in the oceanic lower boundary condition appears to be necessary, in addition to the higher model resolution, to enhance the simulation also in the PAC sector. This suggests the possibility that blocking in the two sectors may be the product of at least partially different dynamical processes. Euro-Atlantic blocking appears to be more the product of nonlinear internal dynamics, while the Pacific seems to be more influenced by the interaction with the sea surface. This latter fact is consistent with the work by Ferranti et al. (1994) which also showed the sensitivity of Pacific blocking to tropical SST anomalies.

Concerning blocking seasonality, the two sectors are characterized by different cycles; blocking is not in any way a winter-only phenomenon in the E-A sector, where the yearly maximum rather takes place in spring. The PAC sector, on the contrary, is characterized by a stronger winter maximum. As for model performances, in the E-A sector all model versions analyzed produced a sufficiently well-shaped annual cycle, the higher resolution integrations also showing an amplitude more comparable

to observations. A shift in time compared to observations was found in the T42 control run of ECHAM3, where the model appears to be approximately one month "too early" in simulating annual minima and maxima of blocking frequency. In the PAC sector the situation is quite different, the reproduction of the annual cycle being generally poor in amplitude and therefore difficult to assess as far as precise timing (phase) is concerned. As could also be expected from blocking frequency diagrams, the GAGO T42 run is the one which gives the best results in the PAC sector.

Turning attention to blocking signatures, i.e. blocked minus zonal composite maps, it is evident that although model behaviour is again different in the two sectors, the main problem of models' representation of sector blocking patterns is connected with their inability to

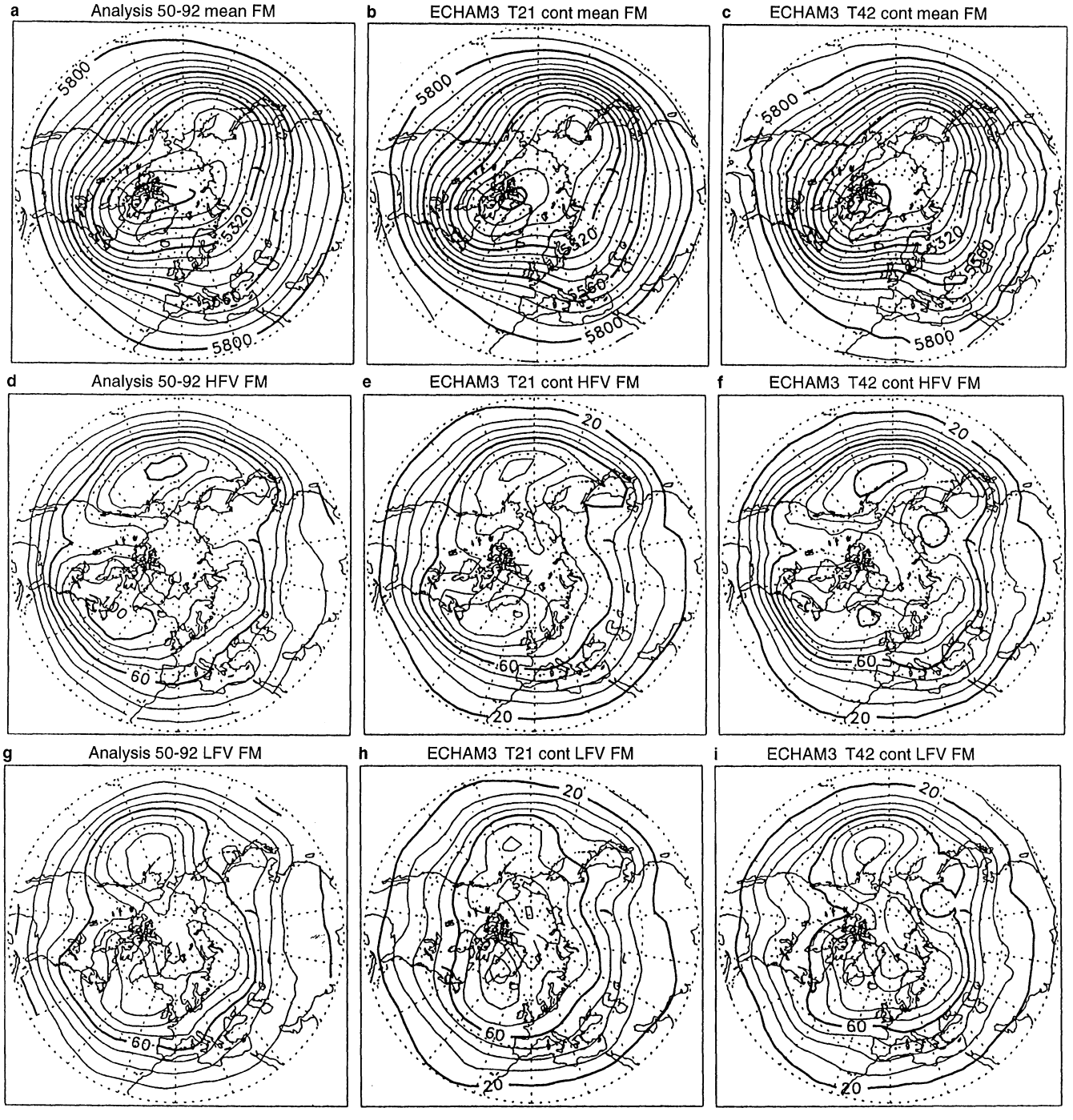

Fig. A1a–i. Mean, high frequency (periods shorter than five days) standard deviation and low frequency standard deviation (periods longer than 5 days) of the 500 hPa GPH field of the control runs and of the 1950–1992 analysis. February–March period. **a**, **b** and **c** contour every 60 m, **d** to **f** contour every 10 m

produce localized signatures. Additional, weaker features are evident and in some cases these are reminiscent of well-known teleconnection patterns.

Blocking length diagrams show that in the EA sector the T21 tends to produce a larger number of shorter blocks than observed, while the T42 is less prone to this error. The situation is different in the Pacific sector, where the performance of the T21 model is comparable to that of the T42. Additionally, the use of observed SSTs rather than climatology does not appear to influence model blocking lifetimes appreciably. An attempt to interpret this bias towards shorter blocks may involve the mechanism of transient eddy forcing, e.g. Green (1977).

From these factors, we can summarize that in addition to the conclusions regarding the performance of ECHAM3, some further evidence of a different nature of the blocking phenomenon in the Euro-Atlantic and Pacific sectors was found. The two sectors appear to be characterized by a different sensitivity of blocking frequencies towards SST model forcing, by a different annual cycle

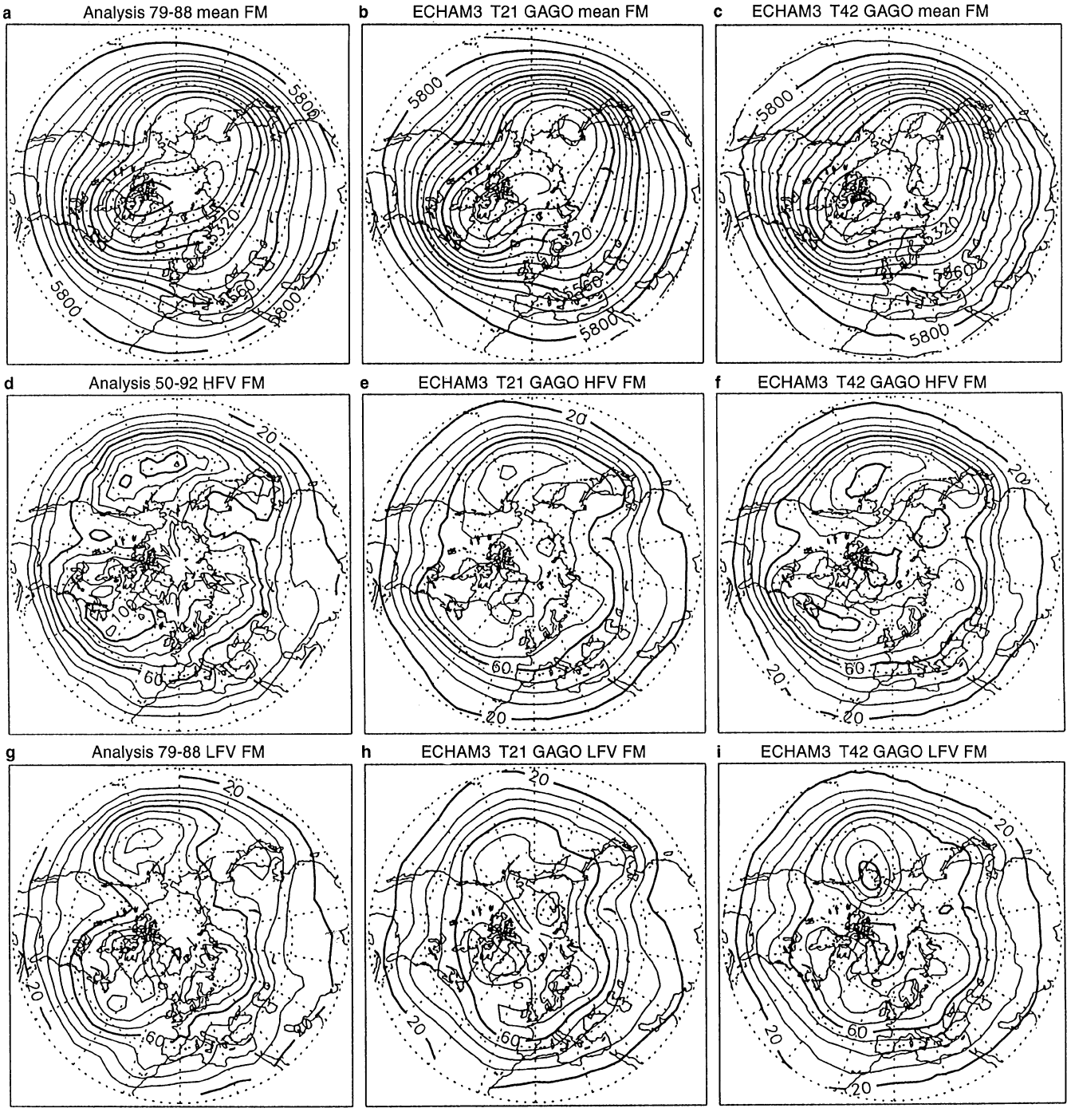

Fig. A2. Analogous to Fig. A2 but for the GAGO runs and for the 1979–1988 analysis

and by a different sensitivity of the distribution of blocking lifetime to model resolution.

Appendix

Figs. A1, A2

Acknowledgements. This work has been partially supported by the CEC EPOCH (C21C) and ENVIRONMENT (Short Term Climate Variability) projects. Elisa Manzini (Max-Planck-Institut für Meteorologie) provided useful comments on an early version of the manuscript. Acknowledgements also go to Jeff Anderson (GFDL), Davide Cesari, Marco Lazzeri and Paolo Ruti (all from ADGB) for the useful exchange of data and ideas. The careful work of two referees has improved substantially the final version of the work.

References

Anderson JL (1993) The climatology of blocking in a numerical forecast model. J Clim 6 : 1041–1056

Austin JF (1980) The blocking of middle latitude westerly winds by planetary waves. Q J R Meteorol Soc 106 : 327–350

Bengtsson L (1980) Review of theories of blocking. In: ECMWF Seminar on Dynamical Meteorology and Numerical Weather Prediction Vol II, pp 235–269

Benzi R, Saltzman B, Wiin-Nielsen AC (eds) (1986) Anomalous atmospheric flows and blocking. Adv Geophys 29 : 439 pp

Blackmon ML, Mullen ST, Bates GT (1986) The climatology of blocking in a perpetual January simulation of a spectral general circulation model. J Atmos Sci 43 : 1379–1405

Brankovic C, Ferranti L (1991) Seasonal integrations with realistic boundary forcing. In: ECMWF Workshop on New Developments in Predictability, pp 305–333

Boyle JS (1992) Sensitivity of dynamical quantities to horizontal resolution in a climate simulation with the ECMWF atmospheric general circulation model (cycle 33). PCMDI Rep 6, Program for Climate Model Diagnosis and Intercomparison, University of California, Lawrence Livermore National Laboratory, Livermore, CA, pp 38

Corti S, Giannini A, Tibaldi S, Molteni F (1997) Patterns of low-frequency variability in a three-level quasi geostrophic model. Climate Dynamics, in press

Charney JG, DeVore JG (1979) Multiple flow equilibria in the atmosphere and blocking. J Atmos Sci 36 : 1205–1216

Dole RM, Gordon ND (1983) Persistent anomalies of the extratropical northern hemisphere wintertime circulation: geographical distribution and regional persistence characteristics. Mon Weather Rev 111 : 1567–1586

Dümenil L, Todini E (1992) A rainfall-runoff scheme for use in the Hamburg climate model. In: O'Kane JP (ed) Advances in theoretical hydrology, a tribute to James Dooge. European Geophysical Society Series of Hydrological Sciences, 1. Elsevier, Amsterdam pp 129–157

Deutsches KlimaRechenZentrum (DKRZ) (1993) The ECHAM3 atmospheric general circulation model. Techn Rep 6, ed the Modellbetreuungsgruppe, DKRZ, Hamburg

Ferranti L, Molteni F, Palmer TN (1994) Impact of localised tropical SST anomalies in ensembles of seasonal GCM integrations. Q J R Meteorol Soc 120 : 1613–1646

Frederiksen JS (1982) A unified three-dimensional instability theory of the onset of blocking and cyclogenesis. J Atmos Sci 39 : 969–987

Gates WL (1991) The validation of atmospheric models. In: Speranza A, Tibaldi S, Fantechi R (eds) Proceedings of the First Demetra Meeting on the Dilemma of Global Warming. Chianciano Terme, Italy, 28 October – 1 November 1991, European Commission, Directorate-General XII, Luxembourg, pp 218–232

Gates WL (1992) AMIP: the Atmospheric Model Intercomparison Project. Bull Am Meteorol Soc 73 : 1962–1970

Green JSA (1977) The weather during July 1976: some dynamical considerations of the drought. Weather 32 : 120–128

Haines K, Marshall JM (1987) Eddy-forced coherent structures as prototypes of atmospheric blocking. Q J R Meteorol Soc 113 : 681–704

Hense A, Kerschgens M, Raschke E (1982) An economical method for computing radiative transfer in circulation models. Q J R Meteorol Soc 108 : 231–252

Hollingsworth A, Tibaldi S, Cubasch U, Brankovic C, T Palmer TN, Campbell L (1986) Mid-latitude atmospheric prediction on time scales of 10–30 days. In: Cattle H (ed) Atmospheric and oceanic variability, R Meteorol Soc, Bracknell, pp 117–151

Hoskins BJ, James IN, White GH (1983) The shape, propagation and mean-flow interaction of large-scale weather systems. J Atmos Sci 40 : 1595–1612

Kaas E (1992) Ultra-low frequency, large scale flow patterns and local blocking of the westerlies in the northern hemisphere winter. PhD thesis, Geophysical Institute, University of Copenhagen

Kaas E, Branstator G (1993) The relationship between a zonal index and blocking activity. J Atmos Sci 50 : 3061–3077

Illari L, Marshall JC (1983) On the interpretation of eddy fluxes during a blocking episode. J Atmos Sci 40 : 2232–2242

Lejenäs H, Økland H (1983) Characteristic of northern hemisphere blocking as determinated from a long time series of observational data. Tellus 35A : 350–362

Mak M (1990) Dynamics of an atmospheric blocking as deduced from its local energetics. Q J R Meteorol Soc 117 : 477–493

May W (1994) On the intraseasonal variability within the extratropics in the ECHAM3 general circulation model. Max-Planck-Institut für Meteorologie, Hamburg, Rep 147

McWilliams JC (1980) An application of equivalent modons to atmospheric blocking. Dyn Atmos Ocean 5 : 43–66

Miyakoda K, Sirutis J (1990) Subgrid scale physics in one month forecasts. Part II: systematic error and blocking forecasts. Mon Weather Rev 118 : 1065–1081

Miller M, Palmer TN, Swinbank R (1989) Parametrization and influence of subgridscale orography on general circulation and numerical weather prediction models. Meteorol Atmos Phys 40 : 84–109

Mullen SL (1986) The local balance of vorticity and heat for blocking anticyclones in a spectral general circulation model. J Atmos Sci 43 : 1406–1441

Palmer TN (1989) Medium and extended range predictability and stability of the Pacific/North American mode. Q J R Meteorol Soc 114 : 691–713

Palmer TN, Tibaldi S (1988) On the prediction of forecast skill. Mon Weather Rev 116 : 2453-2480

Palmer TN, Shutts GI, Swinbank R (1986) Alleviation of a systematic westerly bias in general circulation and numerical weather prediction models through an orographic gravity wave drag parametrization. Q J R Meteorol Soc 112 : 1001–1039

Ponater M, Konig W, Sausen R, Sielmann F (1994) Circulation regime fluctuations and their effect on intraseasonal variability in the ECHAM climate model. Tellus 46A : 265–285

Rex DR (1950a) Blocking action in the middle troposphere and its effect upon regional climate. I. An aerological study of blocking action. Tellus 2 : 169–211

Rex DR (1950b) Blocking action in the middle troposphere and its effect upon regional climate. II. The climatology of blocking action. Tellus 2 : 275–301

Roeckner E, Arpe K, Bengtsson L, Brinkop S, Dümenil L, Esch M, Kirk E, Lunkeit F, Ponater M, Rockel B, Sausen R, Schlese U, Schubert S, Windelband M (1992) Simulation of the present day climate with the ECHAM model: Impact of model physics and resolution. Max-Planck-Institut für Meteorologie, Hamburg, Report n93

Sausen R, König W, Sielmann WF (1993) Analysis of blocking events from observations and ECHAM model simulations. Tellus 47A : 421–438

Shutts GJ (1983) The propagation of eddies in diffluent jetstreams: eddy vorticity forcing of blocking flow fields. Q J R Meteorol Soc 109 : 737–761

Shutts GJ (1986) A case study of eddy forcing during an Atlantic blocking episode. Adv Geophys 29 : 135–161

Tibaldi S, Molteni F (1990) On the operational predictability of blocking. Tellus 42A : 343–365

Tibaldi S (1993) Low frequency variability and blocking as diagnostic tools for global change models. In: Shukla J (ed) Prediction of interannual climate variations. NATO-ASI series 1, vol 6, Springer-Verlag, Berlin Heidelberg New York, pp 173–182

Tibaldi S, Palmer TN, Brankovic C, Cubasch U (1991) Extended range predictions with ECMWF models: influence of horizontal resolution on systematic error and forecast skill. Q J R Meteorol Soc 116 : 835–466

Tibaldi S, Tosi E, Navarra A, Pedulli L (1994) Northern and Southern Hemisphere seasonal variability of blocking frequency and predictability. Mon Weather Rev 122 : 197–200

Tibaldi S, Ruti P, Tosi E, Maruca MM (1995) Operational predictability of winter blocking. Ann Geophys 13 : 305–317

Tiedtke M (1989) A comprehensive mass flux convection scheme for cumulus parametrization in large-scale models. Mon Weather Rev 117 : 1779–1800

Tracton MS (1990) Predictability and its relationship to scale interaction processes in blocking. Mon Weather Rev 118 : 1666–1695

Tracton MS, Mo K, Chen W, Kalnay E, Klister R, White G (1989) Dynamical extended range forecasting (DERF) at the National Meteorological Center. Mon Weather Rev 117 : 1604–1635

Tung KK, Lindzen RS (1979) A theory of stationary long waves, I. A simple theory of blocking. Mon Weather Rev 107 : 714–734

Vautard R, Legras B (1988) On the source of midlatitude low frequency variability: nonlinear equilibration of weather regimes. J Atmos Sci 45 : 2845–2867

WMO (1991) Report of the Sixth Session of the CAS/JSC Working Group on Numerical Experimentation. WCRP Rep 53, WMO/TD Rep 405